Effects of the Molecular Structure of Impact Modifier and Compatibilizer on the Toughening of PBT/SBS/PS-GMA Blends

L. B. Canto, E. Hage Jr., L. A. Pessan

Department of Materials Engineering, Federal of São Carlos University, Via Washington Luiz, Km 235, 13.565-905, São Carlos-SP, Brazil

Received 3 December 2005; accepted 18 April 2006
DOI 10.1002/app.24721
Published online in Wiley InterScience (www.interscience.wiley.com).

ABSTRACT: This work aims at studying the toughening process of poly(butylene terephthalate) (PBT) through its blends with styrene-butadiene-styrene block copolymers (SBS), in the presence of poly(styrene-*ran*-glicydil methacrylate) (PS-GMA) as reactive compatibilizer. High values of impact strength were attained for PBT/SBS blends without the compatibilizer; however, this improvement is achieved for blends with SBS having similar viscosity compared to PBT, at high SBS content (40 wt %) and for blends prepared under specific processing conditions. The efficiency of the *in situ* compatibilization of PBT/SBS blends by PS-GMA was found to be strongly dependent on the SBS and PS-GMA molecular characteristics. Better compatibilizing results were observed through fine phase morphologies and lower ductile to brittle transition temperatures (DBTT) as the interfacial interaction and stability of the *in situ* formed compatibilizer are maximized, that is, when the miscibility between SBS and PS-GMA and reaction degree between PBT and PS-GMA are maximized. For the PBT/SBS/PS-GMA blends under study, this was found when it is used the SBS with higher polystyrene content (38 wt %) and with longer PS blocks (M_w = 20,000 g mol^{-1}) and also the PS-GMA with moderate GMA contents (4 wt %) and with molecular weight similar to the critical one for PS entanglements (M_c = 35,000 g mol^{-1}). © 2006 Wiley Periodicals, Inc. J Appl Polym Sci 102: 5795–5807, 2006

Key words: reactive compatibilization; PBT/SBS; PS-GMA

INTRODUCTION

Polybutylene terephtalate (PBT) is an important engineering thermoplastic that associates good mechanical properties such as stiffness, hardness, and abrasion resistance with good chemical resistance, electrical insurance, and fast crystallization kinetics from the melt. These characteristics make PBT very useful for manufacturing injection-molded articles for domestic, electrical, and automotive applications where the above-mentioned characteristics are required.[1] However, PBT has relatively high unnotched impact strength, but its notched impact strength is low and gives brittle fracture.[2]

Attempts to enhance the failure behavior of semicrystalline thermoplastics like PBT were made by adding a rubbery phase to the polymer, which induces specific yielding of the rubber-modified PBT and increases substantially the energy necessary for its fracture.[3] These materials represent the class of polymer blends and are usually produced by the mixture of the polymers in the melt state.

Rubber-modified polymers are immiscible and yield multiphase systems. The corresponding impact performance is strongly determined by the phase morphology, which depends on composition, rheological, and physical characteristics of the components, relative compatibility, and nature and intensity of mixing.[4–7] Hence, to optimize the blend performance, it is important to control the phase morphology of the system, which can be achieved by selecting the characteristics of the components of the blends and the mixing conditions. More recently, *in situ* compatibilization was used to control and stabilize polymer blend phase morphology.[8] The copolymer molecules generated *in situ* tend to located at the blend components interface reducing the interfacial tension[9–11] and suppressing coalescence of the disperse phase.[12,13] Consequently, compatibilization results in a fine and more stable dispersion of a minor and/or high viscous blend component in the matrix. Compatibilizers also promote interfacial adhesion, which improves stress transfer between the blend phases.[14–17]

Highly tough PBT blends were obtained using acrylonitrile-butadiene-styrene (ABS) elastomers,[18,19] acrylonitrile-EPDM-styrene (AES) elastomers,[20] and styrene-butadiene-styrene block copolymers (SBS),[19]

Correspondence to: L. A. Pessan (pessan@power.ufscar.br).
Contract grant sponsors: Sao Paulo State Research Funding Agency (FAPESP) and the Brazilian Federal Research Funding Agencies CNPq and FINEP.

© 2006 Wiley Periodicals, Inc.

among others. SBS block copolymers can associate high rubber contents and low melt viscosity, which represents an additional advantage compared to the ABS and AES. The characteristics of ABS and AES make the ultimate viscosity of PBT/ABS and PBT/AES blends very high, which causes difficulties in the injection molding step of these systems. Compatibilized PBT/ABS[19,21-25] and PBT/AES blends,[26] i.e., blends with improved impact properties and more stable phase morphology within a large processing range were obtained using poly (methyl-methacrylate-*ran*-glycidyl methacrylate) (MMA-GMA) reactive copolymers as *in situ* compatibilizers. For PBT/SBS blends, however, compatibilization has still not been established.

Poly(styrene-*ran*-glycidyl methacrylate) (PS-GMA) is a potential candidate to compatibilize PBT/SBS blends since it can react with PBT[27,28] as well as interact with the styrene phase of SBS block copolymer.[29] Specific studies in literature found that (PS-GMA) copolymers are effective to compatibilize blends of PBT and polystyrene homopolymer (PS).[27,28] The PS-GMA, which is miscible with the PS phase, can react with PBT end groups to form PBT-*graft*-PS-GMA compatibilizer molecules at PBT/PS interface. However, in our work, the interaction of PS-GMA with SBS block copolymers is different compared to its interaction with PS homopolymer. According to a previous study,[29] the amount of PS-GMA capable of solubilizing into the PS domains of the SBS copolymer depends on the ratio between the molecular weight of the PS-GMA and the molecular weight of the PS block of the SBS copolymer, besides the GMA content of PS-GMA as well. The miscibility of PS-GMA in SBS is higher when it is used PS-GMA with lower molecular weight and lower GMA content and/or SBS with higher PS content and longer PS blocks as well.

Based on the discussion made earlier and on the complexity of the PBT/SBS/PS-GMA system showed earlier, it is interesting to investigate the effects of the addition of different types of SBS with varying molecular structure, PS content, and PS block molecular weight, as impact modifiers for PBT and also to explore the effects of addition of different PS-GMA copolymers with different GMA content and molecular weight, on the compatibilization of PBT/SBS blends.

EXPERIMENTAL

Materials

Table I shows the materials used in this work. The PBT is a commercial grade (Valox 315) supplied by General Electric South America. The PBT number average molecular weight (M_n) was calculated to be 36,000 g mol^{-1} [30] based on intrinsic viscosity (IV) determinations in solution of phenol and tetrachloroethane (60/40 volume ratio) at 30°C using the Mark-Houwink-Sakurada relationship ($IV = 1.166 \times 10^{-4} M_n^{0.871}$). The end acid groups [COOH] were calculated to be 80×10^{-6} mol g^{-1} [30] using the Pohl end-group titration method by which PBT solutions in benzyl alcohol/chloroform were titrated by solutions of NaOH in benzyl alcohol.

Three commercial grades of SBS with different molecular characteristics were used in this study and are designed by their molecular weight, polystyrene content and bulk morphology. These SBS materials are essentially triblock copolymers and were obtained from various sources. The SBS copolymers KD1152, VECTOR D6348, and TR1091 were supplied, respectively, by the companies Kraton Polymers, Dexco Polymers, and Petroflex S.A. The SBS

TABLE I
Molecular Characteristics of Polymers Used in This Work

Designation used in this work	Composition[a]	Molecular weight (M_n g mol^{-1})	Molecular weight (M_w g mol^{-1})	Order–disorder transition temperature (T_{ODT})	Haake torque (N m) at 220°C after 3 min
PBT	–	36,000	–	–	12
SBS KD1152	72/28	95,000	$M_w/M_n \cong 1$	240	7
SBS VECTOR	61/39	63,000	$M_w/M_n \cong 1$	200–220	4
SBS TR1091	62/38	105,000	$M_w/M_n \cong 1$	> 240	22
PS-GMA5 18K	4.4	8,240	18,060	–	–
PS-GMA5 26K	4.4	12,150	26,000	–	–
PS-GMA5 33K	4.2	15,950	32,670	–	–
PS-GMA5 63K	5.0	33,140	63,180	–	–
PS-GMA0 26K	0	11,810	23,510	–	–
PS-GMA1 26K	1.1	12,750	26,260	–	–
PS-GMA2 26K	2.1	12,440	26,080	–	–
PS-GMA10 26K	10.2	11,330	25,760	–	–

[a] Compositions of SBS are given in PB/PS (wt %/wt %) determined by FTIR; Compositions of PS-GMA are given in GMA content (wt %) determined by titration.

molecular characterization is presented elsewhere.[31] The SBS molecular weights were determined by size exclusion chromatography (SEC) analysis through a calibration curve based on monodispersed polystyrene standards, and the SBS molecular weights relative to the polystyrene standards were adjusted using a correction factor described in ASTM D 3593 method. The PS and PB contents of the SBS were determined by FTIR, using a calibration curve based on PS and PB standards. The SBS order–disorder transition temperatures (T_{ODT}) were obtained via linear-viscoelastic oscillatory measurements performed on a Rheometric Scientific SR200 cone and plate rheometer. The dynamic elastic and loss shear moduli, G' and G'', were measured as a function of frequency (0.1 to 100 rad/s) at temperatures ranging from 140 to 240°C.

The PS-GMA reactive copolymers were prepared by suspension polymerization using a protocol adapted from the literature.[27] SEC determined the PS-GMA molecular weights through a calibration curve based on monodispersed polystyrene standards. To control the molecular weight of the PS-GMA, different amounts of benzyl peroxide (BPO) were used as initiator during polymerization. The GMA contents in the PS-GMA were determined by titration, according to previous report,[32] which was controlled using appropriate amounts of styrene and GMA monomers during polymerization. Along the text, the first number after the PS-GMA refers to the GMA weight fraction whereas the second number followed by letter k designate the PSGMA molecular weight (in thousands).

The rheological behavior of each material was characterized by torque rheometry (using a HAAKE Rheomix 600p), at 220°C and 50 rpm, with an 80% partially filled chamber. The level of torque registered for each material was taken after 3 min of mixing.

Methods

Characterization of reactions between PBT and PS-GMA

The extent of reaction between PBT and PS-GMA was investigated by torque rheometry tests and dynamic mechanical thermal (DMTA) analyses. PBT and PS-GMA mixtures with the composition 97/3 (wt/wt) were prepared in a torque rheometer (Haake 600p), with a capacity of 69 cm^3 and at chamber temperature of 220°C, rotor speed of 50 rpm, and using 80% of the capacity of the chamber. Dynamic mechanical analysis of PBT/PS-GMA mixtures were carried out on injection-molded Izod bars, premixed in a twin screw extruder (see next section), using a Polymer Laboratories DMTA under two points bending mode, at deformation amplitude of 0.01%, at a frequency of 1 Hz, and a heating rate of 3°C min^{-1}.

Preparation and characterization of PBT/SBS and PBT/SBS/PS-GMA blends

PBT/SBS/PS-GMA blends with different types of SBS (VECTOR, KD1152 and TR1091), different levels of SBS (0, 20, 30, and 40 wt %) and with different types of PS-GMA (5.0 wt %) were prepared in a modular Baker and Perkins ($L/D = 25$ with $D = 19$ mm) intermeshing corotating twin-screw extruder. The screw configuration that was employed comprises two staggered kneading blocks separated by a conventional conveying section. The set upstream contains 12 elements at 30°, 60°, and 90°, while the set downstream involves eight disks at 60°. The barrel temperature was set at 220°C (or 240°C) and the screws rotated at a frequency of 170 rpm. The premixed blend components were incorporated in the machine by a volumetric feeder set at 1.0 kgh^{-1}.

Izod impact bars were prepared in an ARBURG 270V injection-molding machine at 240°C (or 260°C) with mold temperature set at 50°C.

Izod impact strength tests were performed on the notched bars, at different temperatures, according to ASTM D256. Each test value was calculated as the average of at least five independent measurements. The standard deviations for each value were also calculated and are shown as error bars in the plots. The ductile to brittle transition temperature (DBTT) of the blends were considered as the inflection point in the curves corresponding to the Izod impact strength data. It is important to mention that these curves were obtained simply by drawing lines connecting the experimental data with the objective of guiding the eyes and not as a result of a statistical fitting.

The phase morphologies of the blends were examined using a PHILIPS CM 120 transmission electron microscope (TEM) at an accelerating voltage of 120 kV. Ultra thin sections were obtained by cryomicrotoming the samples using a REICHERT ULTRACUT FC S microtome at −60°C. Sections were made perpendicular to the flow direction for the extrudate samples and injection-molded bars. 50 nm thick sections were stained with OsO_4 vapor for 15 h before examination. The rubbery phase of SBS appears as dark areas, whereas the PS phase of SBS appears as gray area in the TEM images.

RESULTS AND DISCUSSION

PBT and PS-GMA reaction studies

Torque rheometry tests

The extent of reaction between the PBT and the series of PS-GMA prepared with different molecular characteristics (molecular weight, GMA content) was studied using torque rheometry tests comparing the

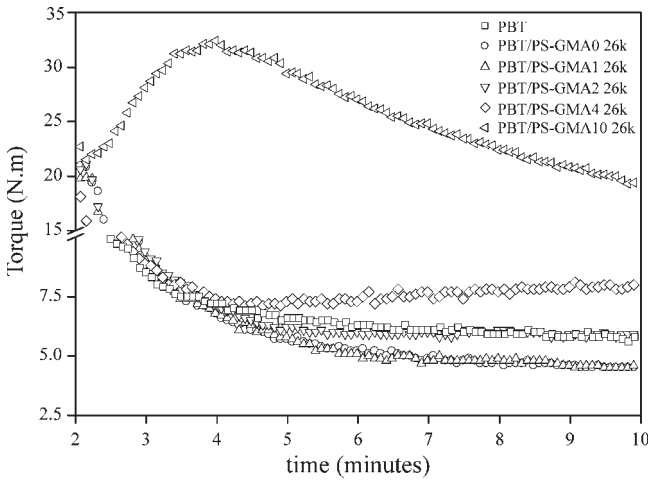

Figure 1 Torque rheometry tests for PBT and PBT/PS-GMA mixtures containing PS-GMA with fixed molecular weight (M_w = 26.000 g mol^{-1}) and different GMA contents (0, 1, 2, 4, and 10 wt % of GMA in PS-GMA).

torque responses between the reactive PBT/PS-GMA mixtures to the nonreactive PBT/PS mixture and to the neat PBT as well. The PS-GMA torque responses were lower than the equipment detection limit, hence, were not measured and can be considered as zero. The level of torque to process each system—proportional to their viscosities—can be considered as indicative of the reaction degrees.

Figure 1 shows torque curves for PBT and PBT/PS-GMA mixtures containing PS-GMA with fixed molecular weight (M_w = 26,000 g mol^{-1}) and different GMA contents (0, 1, 2, 4, and 10 wt % of GMA in PS-GMA). For nonreactive PBT/PS-GMA mixtures (PBT/PS), the level of torque was lower compared with that of neat PBT, which is due to the low viscosity of neat PS in addition to its incapability of reacting with PBT. For reactive mixtures of PBT and PS-GMA, however, the level of torque was higher than that of nonreactive PBT/PS ones and the torque increased with increasing the GMA content in PS-GMA.

The effect of increase of the viscosity observed for mixtures PBT/PS-GMA was attributed to the possible formation of more viscous PBT-*graft*-PS-GMA molecules through the reaction between the PBT end groups and epoxide groups of PS-GMA. According to the literature,[33] interfacial reactions were considered the main reactions between PBT and PS-GMA; however, one cannot discard the occurrence of cross-linking reactions.

Figure 2 shows torque curves for PBT and PBT/PS-GMA mixtures containing PS-GMA with similar GMA contents (4 wt % of GMA in PS-GMA) and different molecular weights (M_w = 18,000; 26,000; 33,000; and 63,000 g mol^{-1}). For this series of mixtures, it was observed that mixtures containing PS-GMA4 with higher molecular weights presented higher levels of torque.

The effects of PS-GMA molecular characteristics on the reaction with PBT can be understood considering the kinetics of interfacial reactions between polymers in molten state. According to the literature,[34–36] these reactions are reaction-controlled and not diffusion-controlled and they can be described by simple second-order kinetics. Thus, the extent of reaction between PBT and PS-GMA depends only on the reactivity and the relative amounts of PBT end groups and epoxide groups in PS-GMA interface. Obviously, the mixture of PBT and PS-GMA with higher GMA contents in PS-GMA is expected to produce more PBT-*graft*-PS-GMA molecules and, hence, generate more viscous systems. On the other hand, the increase of the torque observed for the mixtures containing PS-GMA with higher molecular weights is caused by the PBT-*graft*-PS-GMA with higher PS-GMA lengths and, hence, higher viscosities.

DMTA

The DMTA analyses of PBT/PS-GMA mixtures gave a better understanding of the reactions occurring in the system as a function of different molecular characteristics of PS-GMA (GMA content and molecular weight).

Figure 3 shows DMTA relaxation spectra for PBT and PBT/PS-GMA mixtures containing PS-GMA with similar molecular weight (M_w = 26,000 g mol^{-1}) and different GMA contents (0, 1, 2, and 4 wt % of GMA in PS-GMA). For these mixtures, the PBT and the PS-GMA glass transition temperatures (T_g) were observed to get closer when the GMA content in

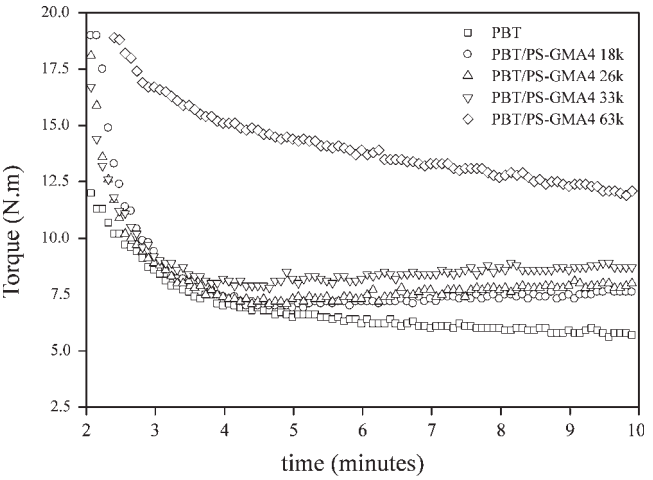

Figure 2 Torque rheometry tests for PBT and PBT/PS-GMA mixtures containing PS-GMA with similar GMA contents (4 wt % of GMA in PS-GMA) and different molecular weights (M_w = 18.000; 26,000; 33,000; and 63,000 g mol^{-1}).

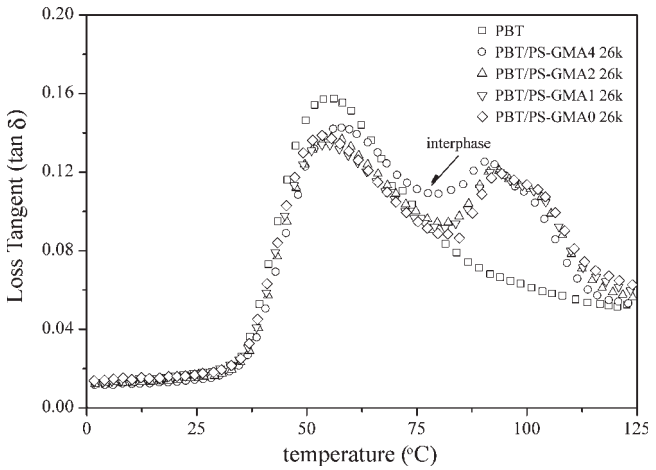

Figure 3 DMTA relaxation spectrum (tanδ versus temperature) for PBT and PBT/PS-GMA mixtures containing PS-GMA with similar molecular weight (M_w = 26,000 g mol^{-1}) and different GMA contents (0, 1, 2, and 4 wt % of GMA in PS-GMA).

PS-GMA increases. The mixture containing PS-GMA with 4 wt % of GMA showed a less pronounced depression in the DMTA curve between the glass transitions of the PBT and of the PS-GMA. This behavior can be understood as indicative of the presence of an interphase consisted of PBT-*graft*-PS-GMA molecules in this system. Obviously, this interphase is more evident for mixtures where larger amounts of PBT-*graft*-PS-GMA are formed, that is, containing higher GMA contents. On the other hand, for the PBT/PS-GMA mixtures containing PS-GMA with similar GMA contents (4 wt % of GMA in PS-GMA) and different molecular weights (M_w = 18,000; 26,000; and 33,000 g mol^{-1}), no significant differences in the DMTA curves was observed, which indicate that similar amounts of PBT-*graft*-PS-GMA are formed independently of the PS-GMA molecular weights.

Izod impact strength and phase morphology of PBT/SBS blends

Effect of SBS type and content on phase morphology and impact behavior

Figure 4 shows the phase morphologies of the PBT/SBS blends containing 30 wt % of different SBS types (VECTOR, KD1152 and TR1091) extruded at 220°C. The SBS phase appears as dark domains in the in TEM photomicrographs due to the Osmium staining. The phase morphologies of extrudate PBT/SBS blends are quite different mainly for the blend with SBSVECTOR where a phase inversion was observed, i.e., PBT was encapsulated by a continuous SBS phase. For blends of PBT with SBS KD1152 and TR1091, however, SBS domains disperse in a PBT matrix can be observed. The PBT/SBS KD1152 blend presents more spherical and homogeneous SBS domains with improved dispersion compared to the PBT/SBS TR1091 blend, which show elongated SBS domains. The phase morphologies shown in Figure 4 can be correlated to the SBS/PBT torque ratio (TR) (Table I). The PBT/SBS KD1152 blend with TR = 0.6 presented the best dispersion; PBT/SBSTR1091 blend with TR = 1.8 showed a bad dispersion when compared with the former, while the PBT/SBS VECTOR blend with TR = 0.3 presented morphology with phase inversion when compared with the morphologies of the other two systems above-mentioned. These behaviors suggest the occurrence of lower and higher TR limits where the deformation and break-up of the SBS domains are more difficult to occur in the extrusion process. Torque ratio also affects the coalescence process. In this case, the lower the viscosity of the minor phase the more intense is the coalescence. The observation of lower and higher viscosity limits most favorable for blends dispersion is in a good agreement with the results obtained by Wu in PET/EPR and PA/EPR blends[37] and also by Favis and Chalifoux in PP/PC blends.[38]

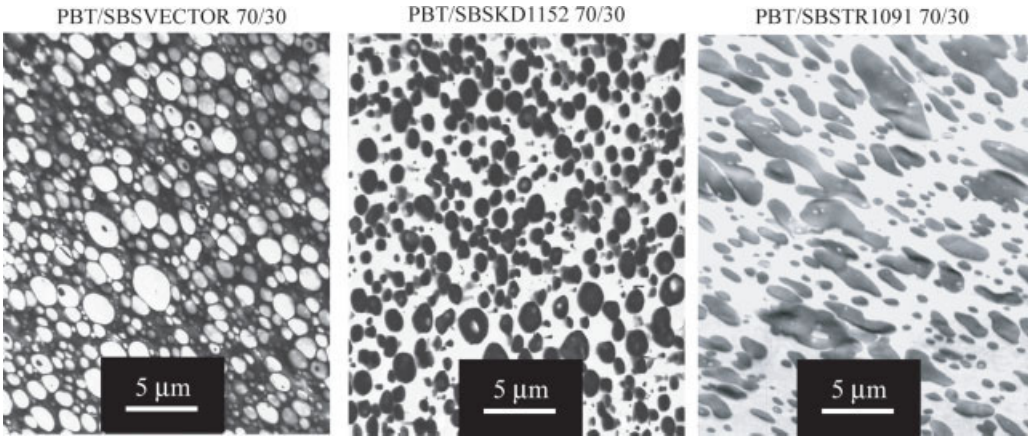

Figure 4 TEM photomicrographs of PBT/SBS 70/30 blends extruded at 220°C as a function of the type of SBS (VECTOR, KD1152, and TR1091). [Color figure can be viewed in the online issue, which is available at www.interscience.wiley.com.]

The phase morphologies for PBT/SBS blends, extruded at 220°C and injection molded at 240°C, as a function of the type and of the content of the SBS in the blends are shown in Figure 5. The type and the content of SBS showed a significant effect on the PBT/SBS phase morphologies. Also, the injection-molding process produces a marked modification of the PBT/SBS 70/30 phase morphologies compared to the extrudate ones (Fig. 4). This fact was attributed to the high instability of SBS particles against coalescence during injection molding process. For the PBT/SBS KD1152 and PBT/SBS TR1091 blends, poorly disperse SBS domains in a PBT matrix were observed; these SBS domains are irregular in shape and increase in size with the increase of their content. In contrast, the PBT/SBS VECTOR blends pre-

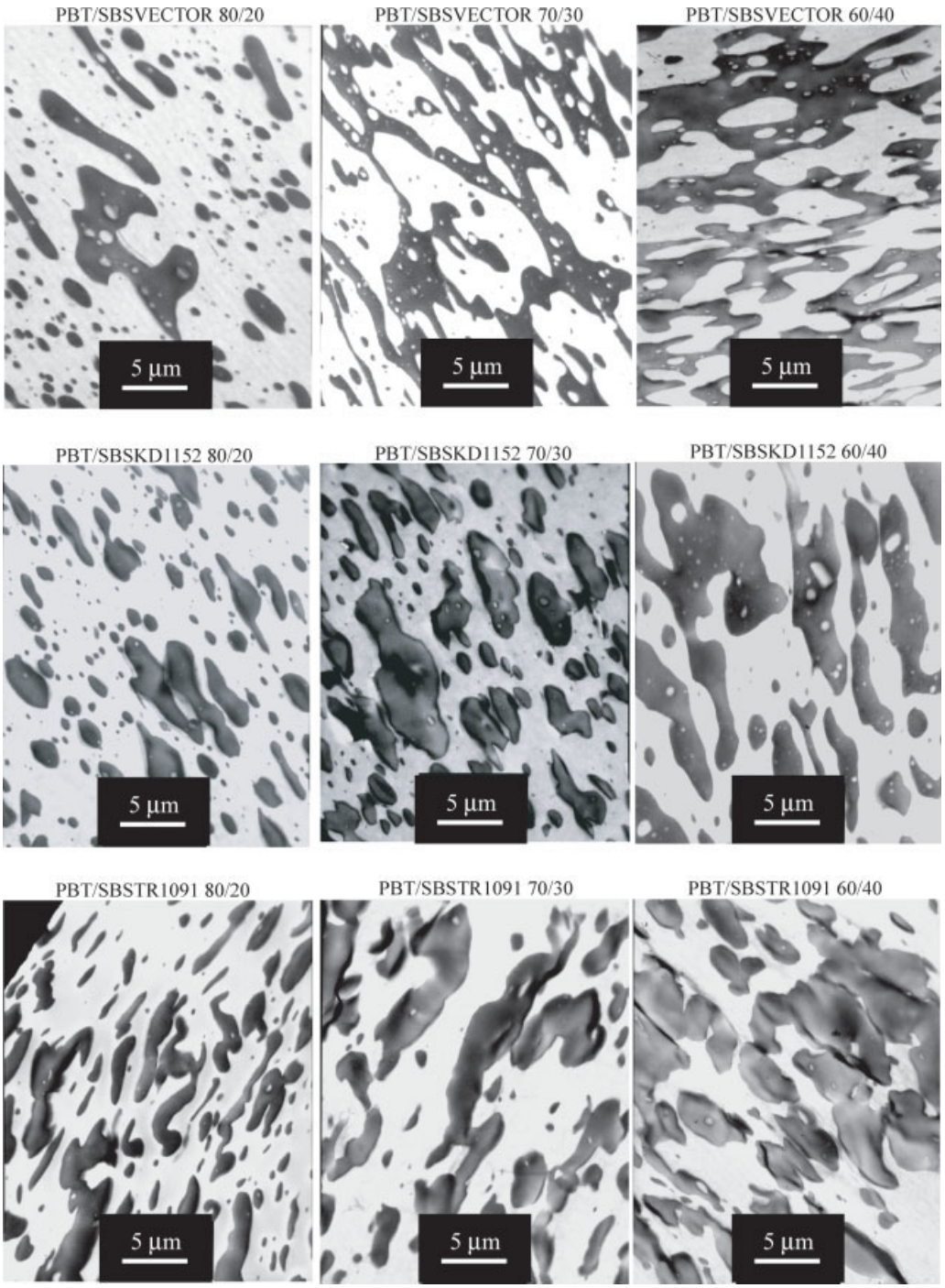

Figure 5 TEM photomicrographs of PBT/SBS blends extruded at 220°C and injection molded at 240°C as a function of the type (VECTOR, KD1152, and TR1091) and the content (0, 20, 30, and 40 wt %) of the SBS. [Color figure can be viewed in the online issue, which is available at www.interscience.wiley.com.]

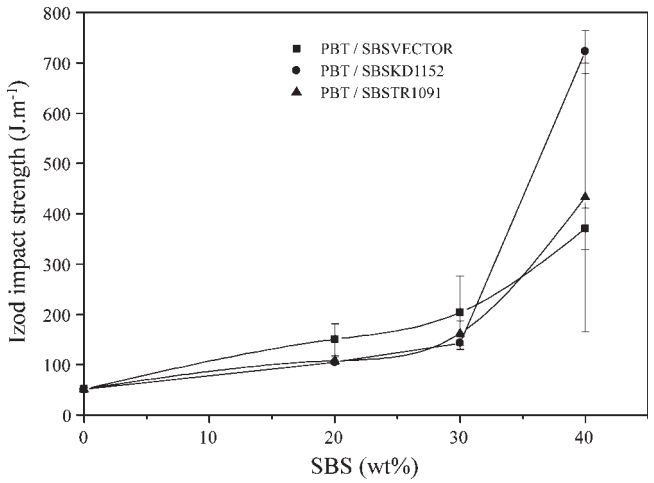

Figure 6 Notched Izod impact strength at room-temperature of PBT/SBS blends as a function of SBS type (VECTOR, KD1152, and TR1091) and SBS content (0, 20, 30, and 40 wt %). Blends extruded at 220°C and injection molded at 240°C.

sented poorly disperse SBS particles in a PBT matrix for the 80/20 composition and cocontinuous phase morphologies for blends containing 30–40 wt % of SBS VECTOR.

Figure 6 shows the room temperature notched Izod impact strength of PBT/SBS blends as a function of the SBS type (VECTOR, KD1152, and TR1091) and the SBS content (0, 20, 30, and 40 wt %). These blends were extruded at 220°C and injection molded at 240°C. The neat PBT fractures in a brittle manner (50 Jm^{-1}) at room temperature, which is a result of its high sensitivity to the notch. The notch tip creates a triaxial stress state that is very favorable to unstable crazes formation, which leads to small plastic deformation around the notch and provides low fracture energy absorption. Addition of SBS results in PBT toughening with impact strength at different levels depending on the type and content of SBS. For PBT/SBS KD1152 60/40 blend, high level of toughness was achieved; this blend shows impact strength of 700 Jm^{-1} in Izod impact tests with highly rough and whitened surface. These observations suggest the occurrence of dilatational process during fracture which, according to studies of deformation mechanisms in rubber toughened PBT,[39] relieves the triaxial stress state in PBT matrix allowing it to be extensively deformed by shear yielding.

The Izod impact strengths obtained for PBT/SBS blends correlate well with their phase morphologies in terms of existence of a critical interparticle distance[40] of SBS domains to succeed in toughening the PBT matrix. As PBT/SBS blends presented poor SBS dispersion, high impact strength are attained for blends with quite high SBS content where the stress fields around neighboring SBS particles can interact considerably, resulting in enhanced shear yielding of PBT and larger energy dissipation.

Effect of SBS type and processing conditions on PBT/SBS impact behavior

The effects of the extrusion and injection-molding temperatures on the notched Izod impact strength of the PBT/SBS blends were evaluated by comparing their ductile to brittle transition temperatures (DBTT), which in turn allow an evaluation of the rubber dispersion in these blends once blends with lower DBTT usually show more disperse phase morphologies. Figures 7–9 show the DBTT of the blends of PBT containing 30 wt % of each type of SBS, VECTOR, KD1152, and TR1091, respectively. The PBT under study presents a DBTT around 70°C[19] and the addition of 30 wt % of any type of SBS reduced considerably the DBTT of PBT/SBS blends. This effect is very common in rubber toughened semicrystalline polymers like PBT and it arises from enhancement of the ability for shear yielding of the semicrystalline matrix.[3] The DBTT of PBT/SBS blends are dependent on the SBS type and on blend thermal processing history. The last characteristic is an indication of PBT/SBS unstable phase morphologies. The injection-molding temperature seems to have the most significant effect on the DBTT of the PBT/SBS blends with SBS disperse phase morphologies, that is, PBT/SBS KD1152 (Fig. 8) and PBT/SBS TR1091 (Fig. 9) but not for cocontinuous PBT/SBS VECTOR blends (Fig. 7). For the blends containing the SBS KD1152 and TR1091, when the molding temperature is increased from 240 to 260°C, the PBT viscosity is reduced, which intensify the coalescence of disperse SBS particles increasing the DBTT of these PBT/SBS blends. On the other hand, for the PBT/SBS VECTOR blends the increase on the molding temperature did not show influence on their cocontinuous phase morphology nor on their DBTT. The literature has demonstrated similar effects for PBT/ABS blends.[21–22]

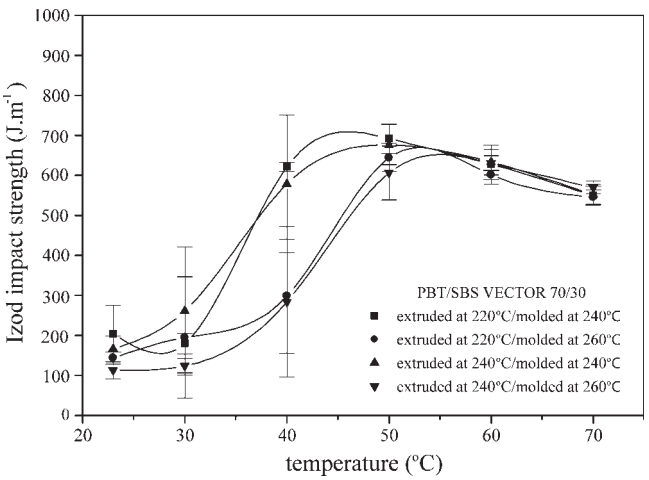

Figure 7 Ductile to brittle transition temperature (DBTT) of PBT/SBSVECTOR 70/30 blends as a function of the extrusion and molding temperatures.

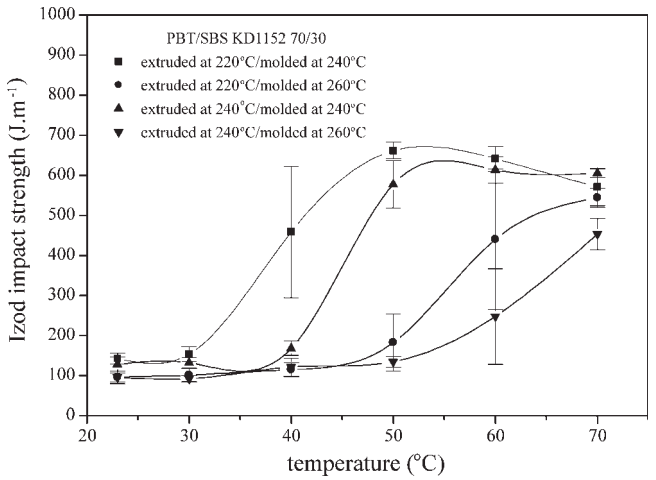

Figure 8 Ductile to brittle transition temperature (DBTT) of PBT/SBSKD1152 70/30 blends as a function of the extrusion and molding temperatures.

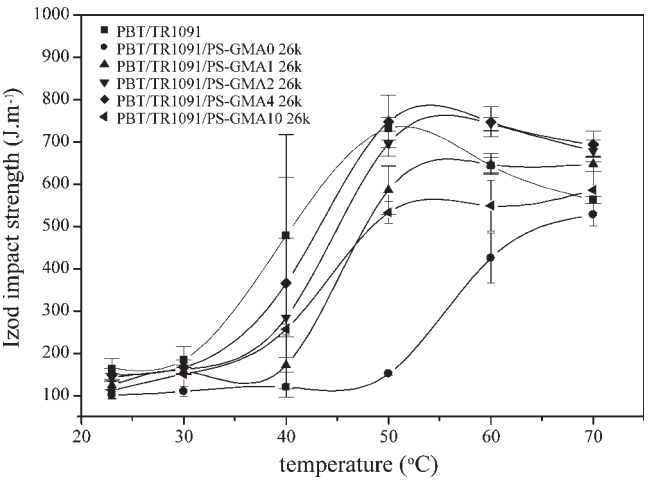

Figure 10 Ductile to brittle transition temperature (DBTT) of PBT/SBSTR1091 70/30 blends and PBT/SBSTR1091/PS-GMA 66.5/28.5/5.0 blends containing PS-GMA with similar molecular weight (M_w = 26,000 g mol^{-1}) and different GMA contents (0, 1, 2, 4, and 10 wt %). Blends extruded at 220°C and injection molded at 240°C.

Izod impact strength and phase morphology of PBT/SBS/PS-GMA blends

Based on the unstable behavior of phase morphology and impact properties of PBT/SBS blends discussed in the last section, it is justified the need for the compatibilization of the PBT/SBS blends to obtain more stable and fine disperse phase morphologies and improved impact properties.

The effect of the molecular structures of the SBS as well as of the PS-GMA on the compatibilization of the PBT/SBS blends were investigated by comparing the ductile to brittle transition temperature (DBTT) and the phase morphologies of the blends PBT/SBS/PS-GMA 66.5/28.5/5.0 with the PBT/SBS 70/30 blends. These blends were extruded at 220°C and injection molded at 240°C.

Figure 10 shows the DBTT of PBT/SBS TR1091/PS-GMA blends containing PS-GMA with similar molecular weight (M_w = 26,000 g mol^{-1}) and different GMA contents (0, 1, 2, 4, and 10 wt %). The DBTT observed for PBT/SBS TR1091/PS-GMA blends were higher compared to the PBT/SBS TR1091 blend. It can also be observed that there is a trend of lowering the DBTT with the increase of the GMA content up to 4 wt % in PS-GMA. The blend with PS-GMA with 4 wt % of GMA showed a DBTT similar to the PBT/SBS blend without PS-GMA. However, for blends with the addition of PS-GMA with 10 wt % of GMA, the DBTT increases again.

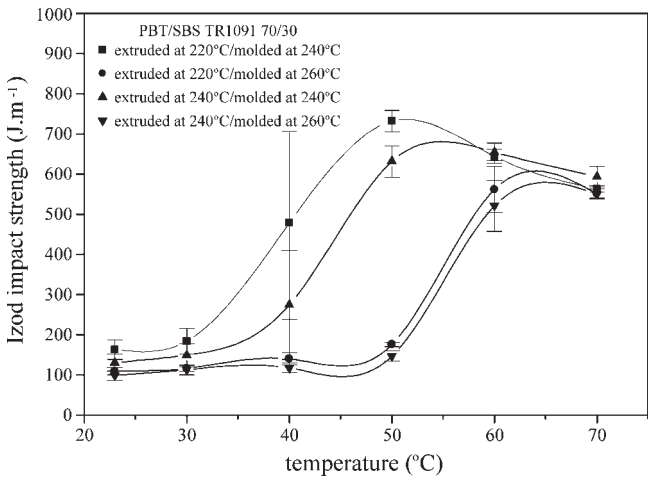

Figure 9 Ductile to brittle transition temperature (DBTT) of PBT/SBSTR1091 70/30 blends as a function of the extrusion and molding temperatures.

Figure 11 shows the effect of the addition of PS-GMA with similar GMA content (4 wt %) and different molecular weights (M_w = 18,000; 26,000; 33,000; and 63,000 g mol^{-1}) on the DBTT of PBT/SBS TR1091/PS-GMA blends. For this series of blends, addition of PS-GMA with higher molecular weights tends to reduce the DBTT. Blends containing PS-GMA with molecular weight of 33,000 and 63,000 g mol^{-1} presented similar behaviors with no significant compatibilization effect on these properties.

Figures 12 and 13 illustrate the effects of addition of the series of PS-GMA with fixed GMA content and different molecular weights on the DBTT of PBT/SBS VECTOR and PBT/SBS KD1152 blends, respectively. These systems presented inferior impact properties with higher DBTT, especially for blends containing the SBS KD1152, compared to the PBT/SBS TR1091/PS-GMA blends.

The phase morphologies for the PBT/SBSTR1091/PS-GMA blends after extrusion at 220°C and also after extrusion at 220°C followed by injection molding (240°C) are shown in Figures 14 and 15, respectively. For extruded blends (Fig. 14), the SBS dispersions are very similar each other, independently of

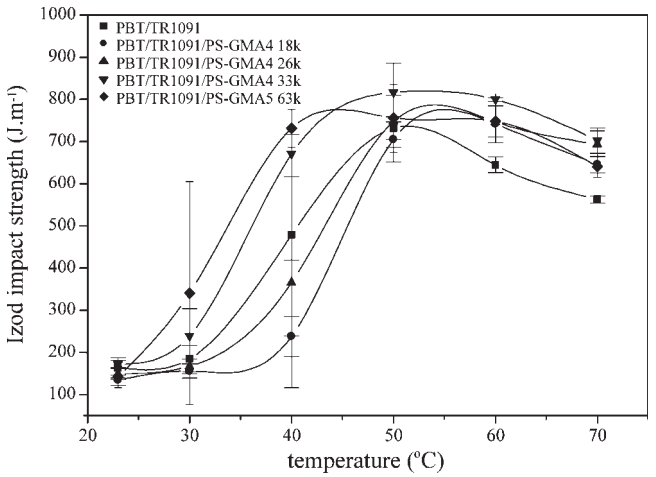

Figure 11 Ductile to brittle transition temperature (DBTT) of PBT/SBSTR1091 70/30 blends and PBT/SBSTR1091/PS-GMA 66.5/28.5/5.0 blends containing PS-GMA with similar GMA content (4 wt %) and different molecular weights (M_w = 18,000; 26.000; 33,000; and 63,000 g mol^{-1}). Blends extruded at 220°C and injection molded at 240°C.

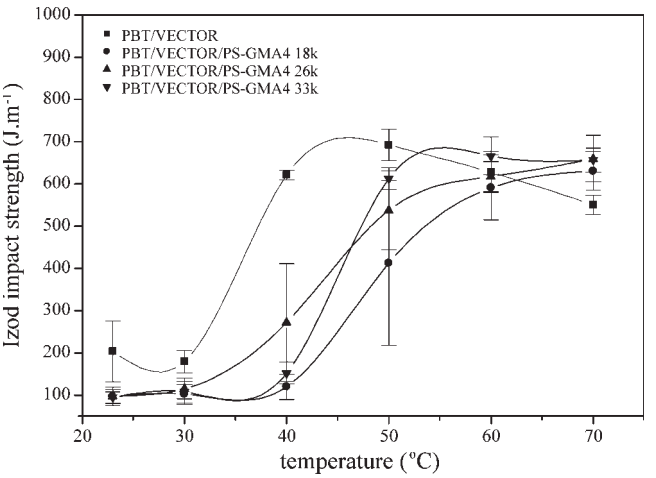

Figure 12 Ductile to brittle transition temperature (DBTT) of PBT/SBSVECTOR 70/30 blend and PBT/SBSVECTOR/PS-GMA 66.5/28.5/5.0 blends containing PS-GMA with similar GMA content (4 wt %) and different molecular weights (M_w = 18,000; 26.000; and 33,000 g mol^{-1}). Blends extruded at 220°C and injection molded at 240°C.

the molecular characteristics of PS-GMA, and they are also slightly poorer than the PBT/TR1091 blend (Fig. 4). After injection molding (Fig. 15), the PBT/TR1091/PS-GMA blends showed coarser phase morphologies compared to the correspondent system that undergone only the extrusion process. The SBS dispersions in injection-molded PBT/TR1091/PS-GMA blends are similar among them and they are slightly better dispersed compared to the equivalent molded PBT/TR1091 blend (Fig. 5).

Figure 16 shows TEM photomicrographs relative to the phase morphologies of each type of SBS (VECTOR, KD1152, and TR1091) in PBT/SBS blends. These blends were extruded at 220°C and injection molded at 240°C. The polybutadiene phase was contrasted dark from polystyrene by Osmium staining. After processing, all SBS presented domain structures of PS and PB with sizes of tenth of nanometers with short-range spatial order. The SBS KD1152 showed polystyrene cylinders disperse into a polybutadiene matrix; the SBS VECTOR presented a lamellar morphology, while the SBS TR1091 showed a mixture of cylindrical and lamellar structures.

As described earlier, the efficiency of the *in situ* compatibilization of PBT/SBS by PS-GMA is strongly dependent on the SBS and the PS-GMA molecular structures. This observation was attributed to dissimilar degrees of interaction between SBS and PS-GMA moiety of the compatibilizer as a function of their different molecular structures as well as different reaction degrees between PBT and PS-GMA molecules. To explain these effects, a simple model was formulated and it is based on the assumption that the SBS block copolymers show microphase separation during the melt processing (extrusion and injection molding) and subsequently during the cooling process. This microphase separation was supposed to be the main responsible for the poor compatibilization results presented by the PBT/SBS/PS-GMA blends. This assumption is basically founded in three aspects:

1. The order–disorder transition temperatures (T_{ODT}) for the studied SBS (Table I) are in the same range of the processing temperatures that were used to prepare the PBT/SBS/PS-GMA blends;

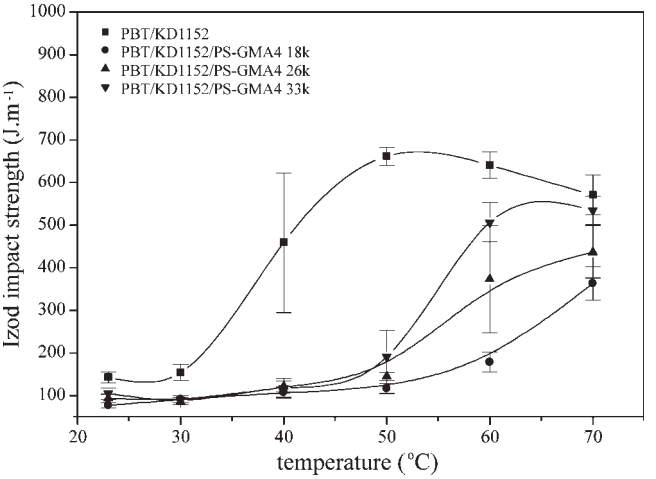

Figure 13 Ductile to brittle transition temperature (DBTT) of PBT/SBSKD1152 70/30 blend and PBT/SBSKD1152/PS-GMA 66.5/28.5/5.0 blends containing PS-GMA with similar GMA content (4 wt %) and different molecular weights (M_w = 18,000; 26.000; and 33,000 g mol^{-1}). Blends extruded at 220°C and injection molded at 240°C.

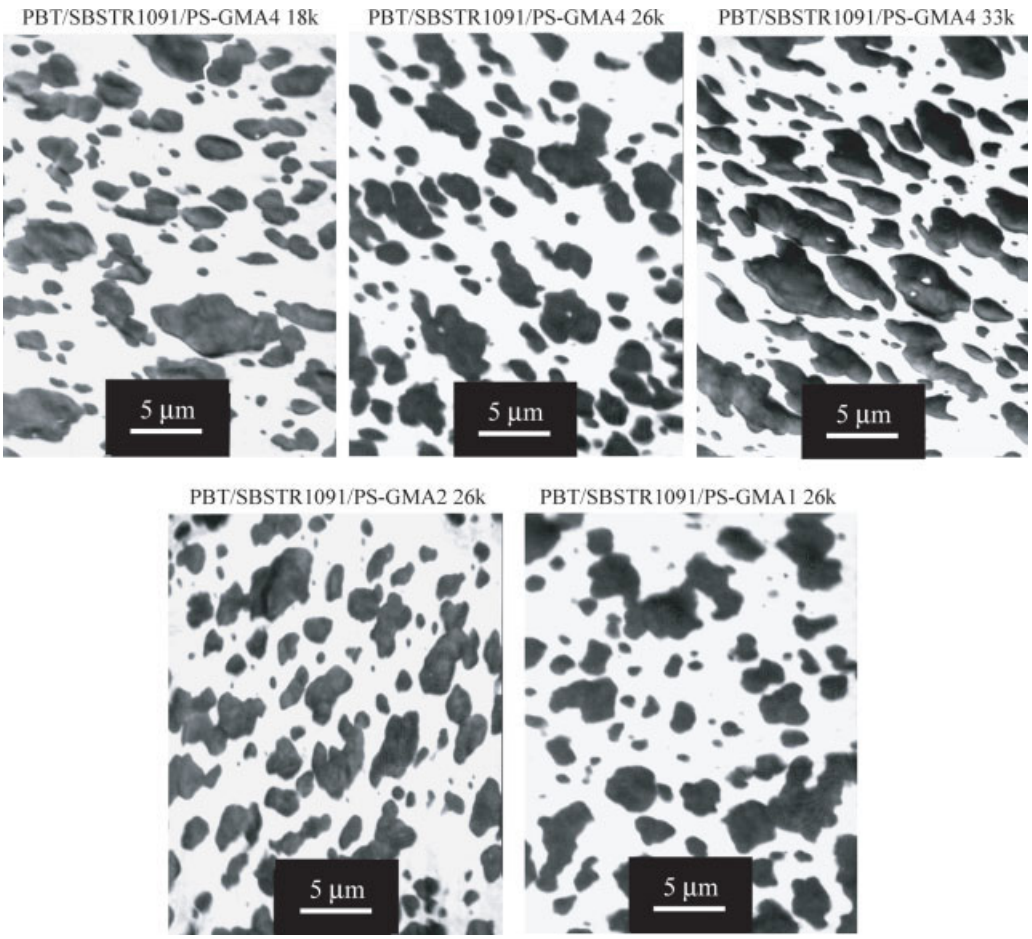

Figure 14 TEM photomicrographs of PBT/SBSTR1091/PS-GMA 66.5/28.5/5.0 blends after extrusion at 220°C containing PS-GMA with different molecular characteristics. [Color figure can be viewed in the online issue, which is available at www.interscience.wiley.com.]

2. The literature showed that the T_{ODT} of SBS block copolymers tends to increase with increasing shear rate[41];
3. The literature showed also that the T_{ODT} of SBS increases with addition of PS with molecular weight at least ¼ of the molecular weight of PS block[42] and it is believed that the same behavior could occur for the SBS/PS-GMA systems.

The microphase separation for the SBS block copolymers that were supposed to occur during blend processing would produce structures similar to that observed after processing (Fig. 16). However, characteristics such as the dimension and range of ordering of the SBS are expected to be a little different due to the processing environment, which produces reordering of SBS domains just below its T_{ODT}.[43]

The SBS microphase separation during the PBT/SBS blends processing was expected to minimize the PBT/PS interfacial area, which is the region where it is expected the effective action of the compatibilizer. Also, the microphase separation would reduce the degree of entanglements between the SBS and the PS-GMA since the molecular weight of PS blocks in SBS (Table I) is below the critical molecular weight for PS entanglements, that is, $M_c = 35{,}000$ g mol^{-1}.[44] The above-mentioned effects together would make the PBT/SBS interface unstable for effective interaction of the compatibilizer with the SBS phase during the blend processing and afterwards; the compatibilizer molecules would be forced to move out from the PBT/SBS interface, which would extremely decrease its efficiency. The literature has demonstrated that the last effect mentioned earlier occur frequently in physically compatibilized blends,[45] but can also occur in some reactive compatibilized blends, especially for highly reactive systems, e.g., systems containing amine and anhydride groups, where the interface is rapidly saturated.[46–49] The fast saturation of the interface makes it unstable, thus the *in situ* formed compatibilizer molecules are pulled-out from the interface creating micelles in the matrix. For PBT/SBS/PS-GMA systems, although the inter-

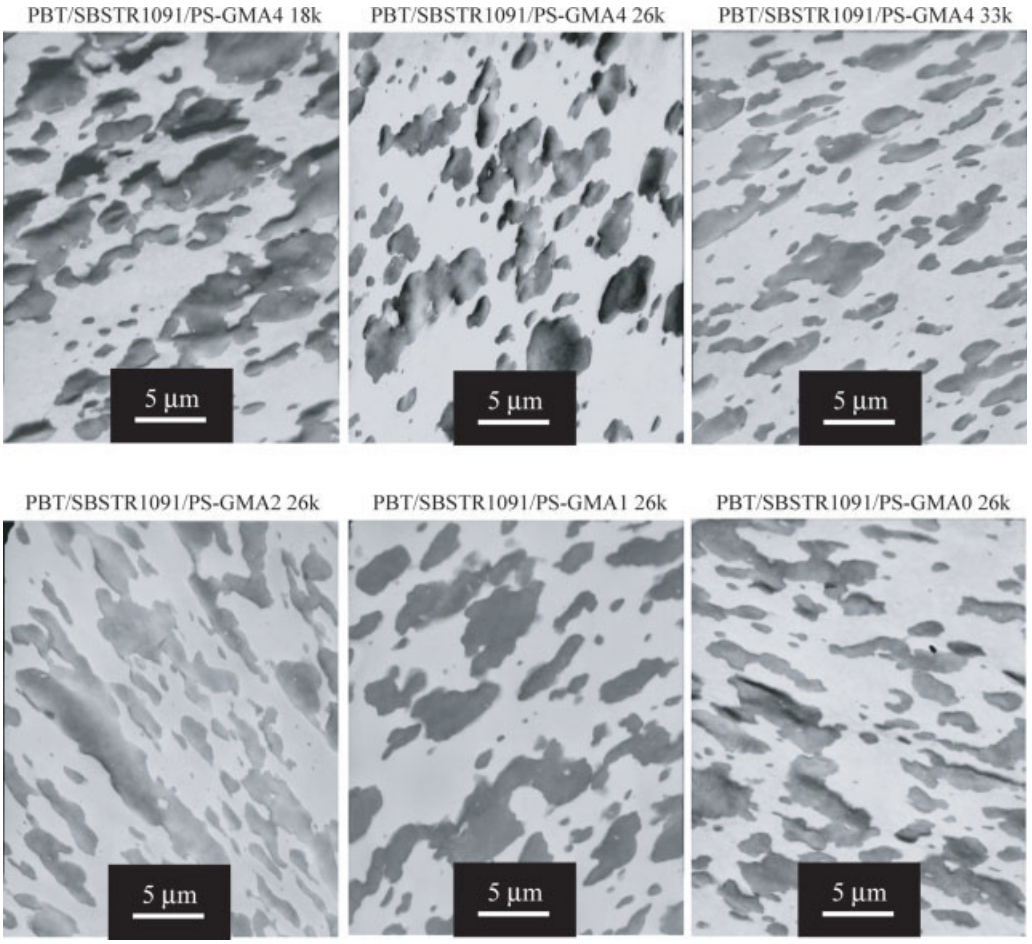

Figure 15 TEM photomicrographs of PBT/SBSTR1091/PS-GMA 66.5/28.5/5.0 blends extruded at 220°C and injection molded at 240°C containing PS-GMA with different molecular characteristics. [Color figure can be viewed in the online issue, which is available at www.interscience.wiley.com.]

face saturation is less probable to occur due to the lower reactivity of COOH and GMA groups compared to the amine/anhydride pair,[36] there is another factor that contributes to the pulling-out effect of the compatibilizer from the interface, which is the weak interaction of the microphase separated SBS phase and the PS-GMA segments from the PBT-*graft*-PS-GMA compatibilizer.

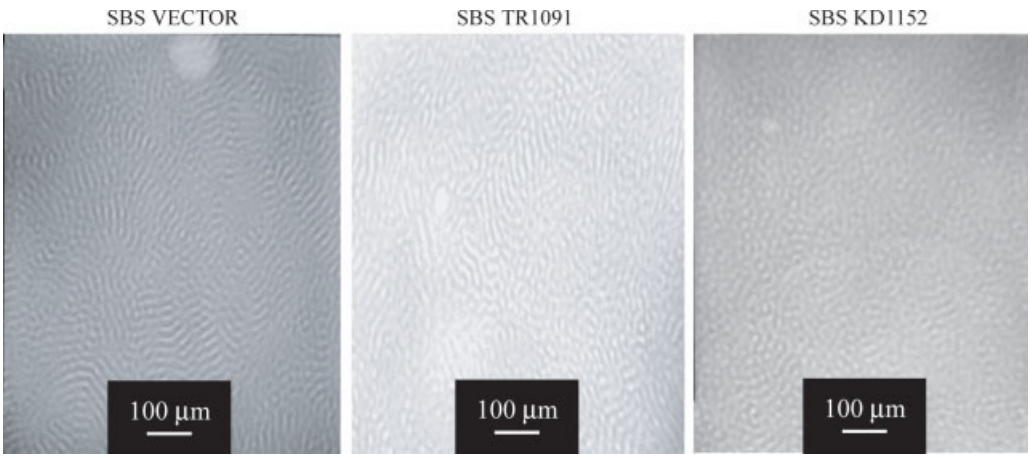

Figure 16 TEM photomicrographs of each type of SBS (VECTOR, KD1152 and TR1091) in PBT/SBS 70/30 blends extruded at 220°C and injection molded at 240°C. [Color figure can be viewed in the online issue, which is available at www.interscience.wiley.com.]

The model presented earlier provides a reasonable explanation for the impact properties and the phase morphologies observed for PBT/SBS/PS-GMA blends as a function of the molecular structures of the SBS and the PS-GMA were used in this study.

Considering the SBS used in this work, the SBS with higher PS content and longer PS block length (TR1091) provides larger interfacial PBT/PS areas with larger capacity to form entanglements with the PS-GMA moiety of PBT-*graft*-PS-GMA compatibilizer. According to a previous study,[29] among the SBS used in this work, the SBS TR1091 has the higher degree of miscibility with the PS-GMA random copolymers studied. It is important to note also that increasing the GMA content in the PS-GMA copolymer increases the amount of the *in situ* formed compatibilizer (Fig. 1), which would favor the compatibilization process. However, the PBT-*graft*-PS-GMA compatibilizer with higher GMA content implies in reduction of their interaction with the PS phase of SBS.[29] Additionally, PS-GMA with higher GMA content tends to produce highly crosslinked PBT-*graft*-PS-GMA molecules (Fig. 1), which in turn, decreases their efficiency as compatibilizers. Therefore, the balance between these opposite effects establishes an optimum GMA content in the PS-GMA copolymer for PBT/SBS compatibilization, which is ca. 4 wt % of GMA in PS-GMA, according to our study. PS-GMA with higher molecular weights would produce PBT-*graft*-PS-GMA compatibilizers with larger segments of PS-GMA, which would improve its ability to make entanglements with the SBS phase; however, higher molecular weight of the *in situ graft* copolymer would reduce its interaction with the PS phase of SBS.[29] Thus, best compatibilization results were observed for the PS-GMA with molecular weight near the critical molecular weight for entanglements for PS, i.e., $M_w = 35{,}000$ g mol^{-1}.

PBT-*graft*-PS-GMA compatibilizer molecules that moved-out of the PBT/SBS interface would also contribute to an increase of the PBT viscosity, which would alter the SBS/PBT torque ratio. For the PBT/SBS TR1091 blend, this change is beneficial for SBS dispersion while for PBT/SBS VECTOR and PBT/SBS KD1152 this change would contribute to SBS coarsening, which also explain the better results for the TR 1091 system. Beside this, the PBT-*graft*-PS-GMA compatibilizer molecules expelled from the interface due to their low interaction with the SBS phase will migrate preferentially to the PBT phase to form micelles, which would make the matrix more brittle. In addition to this effect, the nonreacted PS-GMA molecules could also contribute to the brittleness of the blends since they would locate preferentially on the SBS phase and make them weak, as suggested by studies in the literature on SBS/PS systems.[50]

Based on these results, it is believed that a more effective compatibilization of the PBT/SBS blends by PS-GMA could be achieved with suitable SBS block copolymers with higher polystyrene content and higher polystyrene molecular weight as well, that is, with higher interaction with the PS-GMA moiety of the PBT-*graft*-PS-GMA compatibilizer.

CONCLUSIONS

Extremely tough PBT/SBS blends showing Izod impact strength around 700 Jm^{-1} can be obtained by adding 40 wt % of the SBS with viscosity similar to the PBT used, as indicated by torque rheometry measurements, and when the PBT/SBS blends are prepared at low temperatures such as extruded at 220°C and injection molded at 240°C. Analysis of the final phase morphologies of the PBT/SBS blends by TEM reveals that variables such as composition, SBS/PBT torque ratio, processing equipment (extrusion or injection molding), and processing temperature define the dispersion of the SBS in the PBT matrix and, hence, its impact properties. The PBT/SBS blends showed very unstable phase morphologies, which point to the need of compatibilization of the system.

The efficiency of the *in situ* compatibilization of PBT/SBS blends by PS-GMA is strongly dependent on the SBS and PS-GMA molecular characteristics. Compatibilization effect in the PBT/SBS blends can be attributed to dissimilar interactions between the SBS blend phase with the PS-GMA moiety of the PBT-*graft*-PS-GMA compatibilizer as well as different reaction degrees between PBT and the PS-GMA molecules. Some observations are associated to SBS microphase separation (domains ordering) during the melt processing (extrusion and injection molding) and afterwards. The molecular structure of the SBS such as its low polystyrene content with small PS block lengths can lead to small PBT/PS interfacial area, which is the region where the effective action of the compatibilizer was expected. Also, it would reduce the degree of entanglements between the SBS and the PS-GMA moiety of the PBT-*graft*-PS-GMA compatibilizer, once the molecular weight of PS blocks in SBS are below the critical molecular weight for PS entanglements.

For the PBT/SBS/PS-GMA systems, the better compatibilizing results, observed through fine phase morphologies and lower DBTT, were obtained when the interfacial compatibilizer interaction is maximized, that is, when the miscibility between SBS and PS-GMA and reaction degree between PBT and PS-GMA are maximized and also when it is generated PBT-*graft*-PS-GMA compatibilizer molecules with higher interfacial stability. For the PBT/SBS/PS-GMA

blends, this was achieved when it is used the SBS with higher polystyrene content (38 wt %) and with longer PS blocks (M_w = 20,000 g mol^{-1}) and PS-GMA with moderate GMA contents ($\sim$ 4 wt %) and with molecular weight similar or above the critical molecular weight for PS entanglements (M_c = 35,000 g mol^{-1}).

References

1. Hourston, D. J.; Lane S. Toughened Polyesters and Polycarbonates; Chapman & Hall: London, 1994.
2. Flexman, E. A.Advances in Chemistry Series, Vol. 79; American Chemical Society: Washington, DC; 1993.
3. Paul, D. R.; Bucknall, C. B.Polymer Blends, Vol. 2: Performance; Wiley: New York, 2000.
4. Paul, D. R.; Bucknall, C. B. Polymer Blends, Vol. 1: Formulation; Wiley: New York, 2000.
5. Paul, D. R.; Newman, S. Polymer Blends; Academic Press: New York, 1978.
6. Utracki, L. A. Polymer Alloys and Blends; Hanser Publishers: Munich, 1990.
7. Paul, D. R.; Barlow, J. W.; Keskkula, H. In: Encyclopedia of Polymer Science and Engineering, Vol. 12: Polymer Blends; Wiley: New York, 1998.
8. Xanthos, M. Reactive Extrusion: Principles and Practice; Hanser Publishers: New Jersey, 1992.
9. Kim, J. K.; Jeong, W. Y. Polymer 2001, 42, 4423.
10. Fleischer, C. A.; Morales, A. R.; Koberstein, J. T. Macromolecules 1994, 27, 379.
11. Jiao, J.; Kramer, E. J.; de Vos, S.; Möller, M.; Koning, C. Polymer 1999, 40, 3585.
12. Macosko, C. W. Macromol Symp 2002, 149, 171.
13. Lyu, S.; Jones, T. D.; Bates, F. S.; Macosko, C. W. Macromolecules 2002, 35, 7845.
14. Boucher, E.; Folkers, J. P.; Hervet, H.; Leger, L.; Creton, C. Macromolecules 1996, 29, 774.
15. Beck Tan, N. C.; Tai, S. K.; Briber, R. M. Polymer 1996, 37, 3509.
16. Cho, K.; Li, F. Macromolecules 1998, 31, 7495.
17. Bernard, B.; Brown, H. R.; Hawker, C. J.; Kellock, A. J.; Russel, T. P. Macromolecules 1999, 32, 6254.
18. Hage, E.; Hale, H.; Keskkula, H.; Paul, D. R. Polymer 1997, 38, 3237.
19. Mantovani, G. L.; Canto, L. B.; Hage, E.; Pessan, L. A. Macromol Symp 2001, 176, 167.
20. Larocca, N. M.; Hage, E.; Pessan, L. A. Polymer 2004, 45, 5265.
21. Hale, W. R.; Pessan, L. A.; Keskkula, H.; Paul, D. R. Polymer 1999, 40, 4237.
22. Hale, W.; Keskkula, H.; Paul, D. R. Polymer 1999, 40, 365.
23. Hale, W.; Lee, J. H.; Keskkula, H.; Paul, D. R. Polymer 1999, 40, 3621.
24. Hale, W.; Keskkula, H.; Paul, D. R. Polymer 1999, 40, 3665.
25. Canto, L. B.; Mantovani, G. L.; Covas, J. A.; Hage, E.; Pessan, L. A. J Appl Polym Sci,to appear.
26. Larocca, N. M.; Hage, E.; Pessan, L. A. J Polym Sci, Part B: Polym Phys 2005, 43, 1244.
27. Kim, J. K.; Lee, H. Polymer 1996, 37, 305.
28. Kim, J. K.; Kim, S.; Park, C. E. Polymer 1997, 38, 2155.
29. Canto, L. B.; Torrianni, I.; Plivelic, T.; Hage, E.; Pessan, L. A. Polym Int, 2006, 55.
30. Mantovani, G. L. Ph.D. Thesis, UFSCar, Sao Carlos-Brazil, 2004.
31. Canto, L. B.; Mantovani, G. L.; deAzevedo, E. R.; Bonagamba, T. J.; Hage, E.; Pessan, L. A. Polym Bull, 2006, 57, 513.
32. Canto, L. B.; Pessan, L. A. Polym Test 2002, 21, 35.
33. Martin, P.; Devaux, J.; Legras, R.; van Gurp, M.; van Duin, M. Polymer 2001, 42, 2463.
34. Guégan, P.; Macosko, C. W.; Ishizone, T.; Hirao, A.; Nakahama, S. Macromolecules 1994, 27, 4993.
35. Shulze, J. S.; Cernohous, J. J.; Hirao, A.; Lodge, T. P.; Macosko, C. W. Macromolecules 2000, 33, 1191.
36. Orr, C. A.; Cernohous, J. J.; Guegan, P.; Hirao, A.; Jeon, H. K.; Macosko, C. W. Polymer 2001, 42, 8171.
37. Wu, S. Polym Eng Sci 1987, 27, 335.
38. Favis, B. D.; Chalifoux, J. P. Polym Eng Sci 1987, 27, 1591.
39. Hourston, D. J.; Lane, S.; Zhang, H. X. Polymer 1991, 32, 2215.
40. Wu, S. Polymer 1985, 26, 1855.
41. Nakatani, A. I.; Morrison, F. A.; Douglas, J. F.; Mays, J. W.; Jackson, C. L. J Chem Phys 1996, 104, 1598.
42. Xie, R.; Li, G.; Liu, C.; Jiang, B. Macromolecules 1996, 29, 4895.
43. Luo, K.; Yang, Y. Macromolecules 2002, 35, 3722.
44. Aarón, S. M. Macromolecules 1986, 19, 426.
45. Macosko, C. W.; Guégan, P.; Khandpur, A. K.; Nakayama, A.; Marechal, P.; Inoue, T. Macromolecules 1996, 29, 5590.
46. Charoensirisomboon, P.; Chiba, T.; Solomko, S. I.; Inoue, T.; Weber, M. Polymer 1999, 40, 6803.
47. Charoensirisomboon, P.; Inoue, T.; Weber, M. Polymer 2000, 41, 4483.
48. Pan, L.; Chiba, T.; Inoue, T. Polymer 2001, 42, 8825.
49. Jeon, H. K.; Feist, B. J.; Koh, S. B.; Chang, K.; Macosko, C. W.; Dion, R. P. Polymer 2004, 45, 197.
50. Adhikari, R.; Michler, G. H.; Godehardt, R.; Ivan'kova, E. M. Polymer 2003, 44, 8041.